THE ASTROPHYSICAL JOURNAL, 611:L45–L48, 2004 August 10

AN EXTINCTION THRESHOLD FOR PROTOSTELLAR CORES IN OPHIUCHUS

DOUG JOHNSTONE,[1,2] JAMES DI FRANCESCO,[1] AND HELEN KIRK[2]
Received 2004 May 30; accepted 2004 June 28; published 2004 July 9

ABSTRACT

We have observed continuum emission at $\lambda = 850$ μm over ~4 deg^2 of the Ophiuchus star-forming cloud using the Submillimeter Common-User Bolometric Array on the James Clerk Maxwell Telescope, producing a submillimeter continuum map 20 times larger than previous Ophiuchus surveys. Our sensitivity is 40 mJy beam^{-1}, a factor of ~2 less sensitive than earlier maps. Using an automated identification algorithm, we detect 100 candidate objects. Only two new objects are detected outside the boundary of previous maps, despite the much wider area surveyed. We compare the submillimeter continuum map with a map of visual extinction across the Ophiuchus cloud derived using a combination of Two Micron All Sky Survey and *R*-band data. The total mass in submillimeter objects is $\approx 50\ M_\odot$ compared with $\approx 2000\ M_\odot$ in observed cloud mass estimated from the extinction. The submillimeter objects represent only 2.5% of the cloud mass. A clear association is seen between the locations of detected submillimeter objects and high visual extinction, with no objects detected at $A_V < 7$ mag. Using the extinction map, we estimate pressures within the cloud from $P/k \approx 2 \times 10^5$ cm^{-3} K in the less-extincted regions to $P/k \approx 2 \times 10^6$ cm^{-3} K at the cloud center. Given our sensitivities, cold ($T_d \approx 15$ K) clumps supported by thermal pressure, had they existed, should have been detected throughout the majority of the map. Such objects may not be present at low A_V because they may form only where $A_V > 15$, by some mechanism (e.g., loss of nonthermal support).

Subject heading: stars: formation

1. INTRODUCTION

Stars must form out of gravitationally bound substructures within a molecular cloud, but how the substructures themselves form is strongly debated. Possible scenarios for this process range from the gradual release of magnetic support (Mestel & Spitzer 1956; Shu 1983; Nakano 1984; Shu et al. 1987; Mouschovias & Ciolek 1999; Basu & Ciolek 2004), leading to a slow, regulated evolution of structure in the cloud, to violent dissipation through interacting waves (Scalo 1985; Mac Low & Klessen 2004 and references therein).

Rotational transitions of molecules have been important for tracing both substructures and motions within molecular clouds. Transitions that probe low densities in clouds [e.g., CO (1–0)] reveal widespread emission. Lines observed over low-density regions are themselves very wide, indicating the presence of nonthermal motions on large scales that are crucial to overall cloud support. Transitions that probe high densities [e.g., NH_3 (1, 1)], however, reveal more localized pockets within clouds, i.e., dense cores. Lines observed in dense cores are narrower than those observed in lower density regions, indicating that nonthermal motions are reduced on smaller scales, with a concomitant reduction of support (Barranco & Goodman 1998; Goodman et al. 1998). Dense cores are typically associated with embedded protostellar objects, suggesting that they are the gravitationally bound substructures from which stars form (Tachihara et al. 2000; Di Francesco et al. 2004).

Although observations of transitions that probe high densities have been a reliable means to investigate the small-scale substructures of molecular clouds related to star formation, observations of submillimeter continuum emission from such regions are an attractive alternative given the high sensitivities such observations have to mass. For example, large-format bolometer arrays on large submillimeter or millimeter telescopes have been used in recent years to map several square parsecs of nearby star-forming molecular clouds, revealing many substructures in high-density regions at high sensitivities and resolution (Motte et al. 1998; Johnstone & Bally 1999; Johnstone et al. 2000b, 2001). In these regions, the detected continuum emission primarily originates from cold dust grains and is almost always optically thin, so continuum maps reveal temperature-weighted column densities. These data have revealed numerous stellar-mass substructures within the molecular cloud cores whose mass distributions have similarities to the stellar initial mass function.

Most of the regions targeted for wide-field submillimeter continuum mapping have been those known previously to contain dense cores and active star formation. Much of the surrounding regions of lower density cloud have been ignored in these maps, in part to maximize sensitivities. Significant information about the development of substructures may exist in these regions, however, but has been overlooked as a result of this bias. For example, investigation of Orion B North (Johnstone et al. 2001) found all the substructure to be confined to the densest molecular core regions but did not have sufficient cloud coverage to provide explicit environmental constraints. To provide an unbiased view of substructures within nearby star-forming molecular clouds, we present here submillimeter continuum and infrared extinction maps of ~4 deg^2 of the Ophiuchus star-forming cloud. These observations are part of a larger project, the CO-ordinated Molecular Probe Line, Extinction, and Thermal Emission (COMPLETE) project (Goodman 2004), to obtain and compare high-quality molecular line, submillimeter continuum, and infrared extinction data over the extents of the nearby Ophiuchus, Perseus, and Serpens star-forming molecular clouds. (These clouds, as well as the Lupus and Chamaeleon clouds and many isolated cores, are being observed extensively as part of the near- to mid-infrared "From Cores to Disks" [c2d] Legacy survey of the *Spitzer Space Telescope* [Evans et al. 2003].) The data presented here represent about half of the entire extent of Ophiuchus that will be

[1] National Research Council of Canada, Herzberg Institute of Astrophysics, 5071 West Saanich Road, Victoria, BC V9E 2E7, Canada; doug.johnstone@nrc-crnc.gc.ca, james.difrancesco@nrc-crnc.gc.ca.

[2] Department of Physics and Astronomy, University of Victoria, P.O. Box 3055, Station CSC, Victoria, BC V8P 1A1, Canada; hkirk@uvastro.phys.uvic.ca.

TABLE 1
NEWLY IDENTIFIED OPHIUCHUS OBJECTS

Name	R.A. (J2000.0)	decl. (J2000.0)	Peak Flux (Jy beam^{-1})	Total Flux (Jy)	Radius (arcsec)	Cloud A_V
H-MM1	16 27 58.3	−24 33 42	0.40	4.2	36	18
I-MM1	16 28 57.7	−24 20 48	0.30	2.7	32	7

NOTE.—Units of right ascension are hours, minutes, and seconds, and units of declination are degrees, arcminutes, and arcseconds.

mapped in the submillimeter for COMPLETE, but already they comprise a map that is an order of magnitude larger than those of Ophiuchus by Motte et al. (1998) or Johnstone et al. (2000b) (albeit at lower sensitivity), and they sample an order of magnitude in column density of the cloud.

In this Letter, we demonstrate that all substructures detected in the Ophiuchus cloud are confined to a small fraction of the submillimeter continuum map. Despite the 20-fold increase in the area of Ophiuchus probed here, only two objects located off the edges of previous maps are detected. No obvious substructures are found below an $A_V = 7$. Moreover, almost all bright submillimeter objects are found in the most opaque, densest part of the cloud where $A_V \geq 15$ mag, although simple models suggest that they would have been detected at our sensitivity throughout most of the map if they existed. Instead, a column density or extinction threshold for substructure formation, and thus star formation, may exist in Ophiuchus and possibly in other molecular clouds.

2. OBSERVATIONS AND RESULTS

The data were obtained using the Submillimeter Common-User Bolometer Array (SCUBA; see Holland et al. 1999) on the James Clerk Maxwell Telescope (JCMT) on Mauna Kea, Hawaii.[3] The area chosen to map consisted of ~4 deg^2 in western Ophiuchus where $A_V > 3$ and includes the well-known cores Oph A, B1, B2, C, and D at its southeastern corner. This area was divided up into 38 square fields each ~400 arcmin^2 in size. Each field was observed over the course of ~1 hr using the "fast scan" observing mode of SCUBA, where the sky is sampled at a Nyquist rate at 850 μm. Each field was scanned six times but at a different chopping amplitude and direction each time. The chop maps were converted into an image by applying the matrix inversion data reduction technique (Johnstone et al. 2000a). Note that by using a chopping secondary to map the region, the data are insensitive to emission on scales larger than a few times the chop throw, i.e., greater than 120″. The fields were observed separately through queue mode scheduling throughout Semester 03A. Since each field was observed at different times and thus under different atmospheric opacities, the sensitivity in the final map varies from field to field but only by a factor of ~1.5. The mean and rms of the 1 σ rms sensitivity for all fields are 40 and 20 mJy beam^{-1}, respectively. Since the JCMT beam is ~14″ FWHM at 850 μm, the final map consists of $\sim 1.9 \times 10^5$ resolution elements, the largest number obtained so far in a single SCUBA map.

Extinctions derived from *R*-band star count data by Cambrésy (1999) were used for the northern half of the map, while those derived from Two Micron All Sky Survey (2MASS; Skrutskie et al. 1997) stellar reddening data by J. Alves et al. (2004, in preparation) as part of COMPLETE were used for the southern half, since public release data were available for those fields. Since 2MASS is an infrared survey, its data are better for probing the highly extincted regions at which the *R*-band extinctions saturate, $A_V \approx 8$. Extinctions derived from *R*-band or 2MASS data over regions in common show a slight difference of less than 1 mag and a tight linear correlation until $A_V \approx 8$.

The resolution of the extinction map depends on the densities of stars used to derive extinctions, but it should be only as low as ~3′ at the highest extinctions (see Lombardi & Alves 2001). The mean and maximum A_V over the surveyed area are 4.2 and 36.2 mag, respectively.

3. DISCUSSION

The $\lambda = 850$ μm continuum map of Ophiuchus can be used to locate the incidences of substructure (i.e., objects of size <120″) in the cloud. To locate objects within the map in an unbiased manner, the Clumpfind algorithm (Williams et al. 1994) was used to identify 100 sources of flux in the map of comparable size to the beam or larger to a 5 σ threshold in peak brightness. All but two of these objects are associated with previously identified substructure in the smaller map of Johnstone et al. (2000b) surrounding the known Oph cores (i.e., A–G; see also Motte et al. 1998) Table 1 lists the names, positions, and fluxes of two objects not previously identified since they lie beyond the edges of earlier continuum maps. They reside in two new cores in Ophiuchus, which we name Oph H and Oph I following Motte et al. (1998). No infrared or X-ray sources toward either core are reported within the SIMBAD database.

Detections of substructure in Ophiuchus allow us to measure their mass and determine their location while the extinction map can be used to estimate the total cloud mass over the same area. The integrated flux from all the substructure in the cloud is 250 Jy. Assuming a dust temperature $T_d = 15$ K, a dust opacity at 850 μm $\kappa_\nu = 0.02$ cm^2 g^{-1}, and a distance of 160 pc to Ophiuchus then 1 Jy $= 0.20$ $M_\odot$ (Johnstone et al. 2000b). Therefore, the amount of mass in substructures detected is ~50 $M_\odot$. From the extinction data and assuming $A_V/N_{\rm H} = 2 \times 10^{21}$, the total amount of mass residing within the map area is ~2020 $M_\odot$. The detected substructures, therefore, only account for ~2.5% of the total amount of mass residing in the map area. Table 2 shows the distribution of these masses with A_V and reveals that significant mass in the substructure is found only at $A_V > 15$ mag.

Cumulative mass calculations may be easily biased by a few massive objects, but this is not the case for our surveyed area. Figure 1 plots the peak flux, total flux, and radius of each identified object versus the A_V at their respective positions. No bright objects are found at $A_V < 15$ despite the large cloud area and mass of that region. A similar result was obtained by Johnstone et al. (2001) for submillimeter objects in Orion B North. At high extinction the total mass in clumps is determined not

[3] The JCMT is operated by the Joint Astronomy Center in Hilo, Hawaii, on behalf of the parent organizations the Particle Physics and Astronomy Research Council in the United Kingdom, the National Research Council of Canada, and the Netherlands Organization for Scientific Research.

TABLE 2
PERCENTAGES OF TOTALS IN RANGES OF EXTINCTION

A_V Range	Cloud Area (%)	Cloud Mass $M_\odot$	Cloud Mass %	Clump Mass $M_\odot$	Clump Mass %	Mass Ratio (%)
0–36	100	2020	100	49.4	100	2.5
0–7	88	1380	68	0	0	0
7–15	9	400	20	3.1	6	0.8
15–36	3	240	12	46.3	94	19

by a single object but by an ensemble, although the Oph A core accounts for one quarter of the mass in compact objects. Comparison of the mass estimation in this Letter with the results of Johnstone et al. (2000b) shows that a significant amount of mass (almost 50% of the submillimeter flux in compact substructure) in the earlier paper was removed by the flattening and filtering techniques, stressing the difficulty in obtaining proper flux baselines for chopped submillimeter maps.

What is the physical significance of having most of the detectable substructure only at $A_V > 15$ mag? A threshold in A_V may need to be exceeded for such objects to form. Alternatively, our observations may not have been sensitive enough to detect substructure in regions of low A_V, e.g., if such objects are larger or less dense than their more embedded brethren. Here, we use a simple model to argue that such objects in locations of low A_V in Ophiuchus should have been detected by our observations if they indeed existed.

Within a molecular cloud, pressure increases with A_V. Following McKee (1989), the pressure at depth r is $P(r) = \pi G \Sigma \Sigma(r)$, where Σ is the mean column density through the cloud and $\Sigma(r)$ is the column density measured inward from the cloud surface to depth r. Near the center of the cloud, $\Sigma(r) \approx \Sigma(s)/2$, where $\Sigma(s)$ is the column density through the cloud at impact parameter s. Thus, pressure in the cloud at depth r can be approximated as $P(r)/k = 1.7 \times 10^4 A_V A_V(s)$ cm^{-3} K, where A_V is the mean extinction through the cloud, $A_V(s)$ is the extinction through the cloud at impact parameter s and adopting $A_V = (\Sigma/\Sigma_0)$ mag where $\Sigma_0 = 4.68 \times 10^{-3}$ g cm^{-2}.

Taking the mean extinction through the cloud as $\bar{A}_V \approx 4$ and the range of measured $A_V = 3$–30 mag, $P/k \approx (0.2–2) \times 10^6$ cm^{-3} K. Although admittedly approximate, the value at the highest extinctions (e.g., the Oph cores) is similar to the 3×10^6 cm^{-3} K found by Johnstone et al. (2000b) from fitting stable Bonnor-Ebert (BE) sphere models (Bonnor 1956; Ebert 1955) to submillimeter objects in the Ophiuchus cores to estimate their masses, internal temperatures, and bounding pressures.

Pressure support for a molecular cloud must come from nonthermal sources such as magnetic fields or turbulence. Most of the previously detected submillimeter objects in Ophiuchus, however, were fitted reasonably well by models of BE spheres supported internally entirely by thermal pressure (Johnstone et al. 2000b). A similar analysis holds true for Orion B North (Johnstone et al. 2001). Note that these fits should not be construed as evidence that the objects are in stable equilibrium, since dynamic entities produced in turbulent clouds can appear like BE spheres (Ballesteros-Paredes et al. 2003). Similarly, the condensed central regions of clumps evolving via ambipolar diffusion approach a similar, albeit flattened, profile (Basu 1997; Basu & Ciolek 2004). The BE sphere model, however, provides a lower limit for the critical mass and column density at which an object will become unstable to gravitational collapse since only thermal pressure is available to act as support.

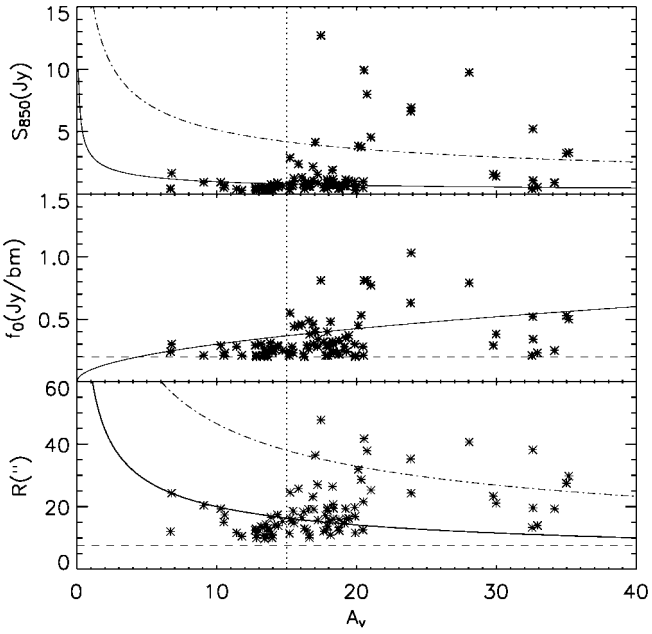

FIG. 1.—Distribution of the observed properties of measured submillimeter clumps with cloud extinction. Panels from top to bottom show for each clump the integrated flux, peak flux, and size. Horizontal dashed lines denote sensitivity and resolution limits, while vertical dotted lines at $A_V = 15$ mag mark the boundary of observed bright objects. The solid lines show the expected evolution with A_V of a BE sphere with a fixed value of λ but only marginally observed at $A_V = 10$ mag (see text). The dash-dotted lines show the upper limit for size and mass of stable BE spheres ($T = 15$ K) as a function of A_V.

Aside from scaling relations, BE spheres are a one-dimensional family of objects defined only by the ratio of central density to surface density, $\lambda = \rho(0)/\rho(R)$, with larger λ implying a greater importance of self-gravity. BE spheres are stable against gravitational collapse if $\lambda < 14$. The mass and density scaling relations of a BE sphere with fixed λ are $M_{\rm BE} \propto P^{-1/2}$ and $\Sigma_{\rm BE} \propto P^{1/2}$.

Can stable objects exist in Ophiuchus where $A_V < 15$ mag and remain undetected in our data? The total submillimeter continuum flux S_{850} associated with a BE sphere is a measure of its mass, weighted by temperature. Thus, for BE spheres with a fixed value of λ, the submillimeter flux as a function of the bounding pressure (assuming that both κ_ν and T remain constant) is $S_{850} \propto P(r)^{-1/2}$ or $S_{850} \propto A_V(s)^{-1/2}$. Similarly, the peak flux f_0 measures the column density and should scale as $f_0 \propto A_V(s)^{1/2}$ and the radius $R \propto A_V(s)^{-1/2}$. The total flux, peak flux, and radius *increase* with increasing λ (until a gravitationally unstable BE sphere is produced).

In Figure 1 the above BE sphere relations are overlaid (*solid line*) on the data to show that nondetections at $A_V = 10$ are incompatible with detections at higher A_V. That is, the lack of significant observed substructure at moderate A_V implies that no objects in these regions are dominated by self-gravity to the extent of those at higher extinction. Since the low A_V regions contain most of the cloud mass, the lack of such detected objects is not due to a lack of material. Also shown in Figure 1 is the upper boundary for stable BE spheres (*dash-dotted line*), assuming that the gas and dust temperature is $T = 15$ K. Unstable objects, those that are capable of collapsing to stars, are found only where $A_V > 17$.

How do these results fit with present theoretical models for star formation? If the dominant mechanism for molecular cloud

support is magnetic pressure mediated by collisions between ions (which couple to the magnetic field) and neutrals, then the timescale for ambipolar diffusion would be long in regions of high ionization, limiting the formation of significant substructure. Crutcher (1999) has shown that the typical magnetic field strength in a molecular cloud is strong enough to supply most, if not all, of the required support against collapse. McKee (1989) demonstrates that in the lower column density regions of molecular clouds, where the extinction to the cloud surface is $A_V < 4$, the interstellar radiation field is capable of maintaining such a high ion fraction. Following this reasoning, the total extinction through regions of the cloud where substructure exists should be $A_V > 8$. This prediction is in excellent agreement with our observations. The somewhat higher threshold A_V that we find is plausibly a result of the nonuniform structure of the molecular cloud. In the regions of high extinction where only cosmic rays are capable of maintaining an ionization fraction, ambipolar diffusion enables the growth of prestellar cores. Recent theoretical calculations show that MHD turbulence may shorten the timescale for ambipolar diffusion within the core by a factor of 3–10 (Fatuzzo & Adams 2002; Zweibel 2002), bringing the ratio of observed cores with and without stars into agreement with their expected lifetimes. Johnstone et al. (2000b) found that approximately half their submillimeter objects in Ophiuchus were associated with infrared emission.[4]

An alternative model for the support of molecular clouds utilizes turbulent motions to supply "nonthermal" pressure support (Mac Low & Klessen 2004). Such motions are observed within molecular clouds via the widths of molecular transitions such as CO (1–0). Indeed, simple virial analysis models indicate that the observed line widths are large enough to provide support of the cloud against collapse, assuming that the nonthermal pressure is isotropic and uniform throughout the cloud (Larson 1981). For Ophiuchus typical line widths are $\Delta V > 1.5$ km s^{-1} (Loren 1989). Within turbulent clouds, the formation of substructure is due to intersecting waves, producing local density maxima, most of which are transient. Ballesteros-Paredes et al. (2003) showed that such features can look similar to BE spheres despite being nonequilibrium objects. It remains to be determined, however, how the formation of substructure depends on local conditions, such as the mean pressure. Naïvely one might expect that these objects should follow a similar scaling relation to BE spheres. Regardless of the exact nature of the scaling, it is difficult to understand how turbulent models can produce the sharp decline in observed objects found in this investigation.

Molecular clouds are likely influenced by both magnetic fields and turbulent motions. The SCUBA observations presented in this Letter suggest an extinction threshold, which is compatible with the predictions of McKee (1989), preventing the formation of relevant substructure over the bulk of the cloud. Thus, observations of submillimeter structure in molecular clouds yield similar conclusions to surveys of the latter-stage embedded stars (Lada & Lada 2003). As with the embedded stars, most if not all of the submillimeter objects reside in highly extincted cores, account for about 20% of the total core mass, and have a stellar-like initial mass function (Motte et al. 1998; Johnstone et al. 2000b). Thus, clustered star formation appears limited to the densest regions of molecular clouds where turbulent motions and enhanced ambipolar diffusion are able to seed an ensemble of prestellar cores.

The research of D. J. has been supported by an NSERC Discovery Grant. H. K. is supported by an NSERC graduate scholarship. The data presented in this Letter were taken as part of queue-based observations at the JCMT. We thank the numerous operators and visiting observers for the observations. This research has made use of the SIMBAD database, operated at the Centre de Données astronomiques de Strasbourg, France.

[4] The high sensitivity of the *Spitzer* c2d survey will likely change this fraction.

REFERENCES

Ballesteros-Paredes, J., Klessen, R. S., & Vázquez-Semadeni, E. 2003, ApJ, 592, 188
Barranco, J. A., & Goodman, A. A. 1998, ApJ, 504, 207
Basu, S. 1997, ApJ, 485, 240
Basu, S., & Ciolek, G. E. 2004, ApJ, 607, L39
Bonnor, W. B. 1956, MNRAS, 116, 351
Cambrésy, L. 1999, A&A, 345, 965
Crutcher, R. M. 1999, ApJ, 520, 706
Di Francesco, J., André, P., & Myers, P. C. 2004, ApJ, submitted
Ebert, R. 1955, Z. Astrophys., 37, 217
Evans, N. J., et al. 2003, PASP, 115, 965
Fatuzzo, M., & Adams, F. C. 2002, ApJ, 570, 210
Goodman, A. A. 2004, in Star Formation in the Interstellar Medium (San Francisco: ASP), in press
Goodman, A. A., Barranco, J. A., Wilner, D. J., & Heyer, M. H. 1998, ApJ, 504, 223
Holland, W. S., et al. 1999, MNRAS, 303, 659
Johnstone, D., & Bally, J. 1999, ApJ, 510, L49
Johnstone, D., Fich, M., Mitchell, G. F., & Moriarty-Schieven, G. 2001, ApJ, 559, 307
Johnstone, D., Wilson, C. D., Moriarty-Schieven, G., Giannakopoulou-Creighton, J., & Gregersen, E. 2000a, ApJS, 131, 505
Johnstone, D., Wilson, C. D., Moriarty-Schieven, G., Joncas, G., Smith, G., Gregersen, E., & Fich, M. 2000b, ApJ, 545, 327
Lada, C. J., & Lada, E. A. 2003, ARA&A, 41, 57
Larson, R. B. 1981, MNRAS, 194, 809
Lombardi, M., & Alves, J. 2001, A&A, 377, 1023
Loren, R. B. 1989, ApJ, 338, 902
Mac Low, M., & Klessen, R. S. 2004, Rev. Mod. Phys., 76, 125
McKee, C. F. 1989, ApJ, 345, 782
Mestel, L., & Spitzer, L., Jr. 1956, MNRAS, 116, 503
Motte, F., Andre, P., & Neri, R. 1998, A&A, 336, 150
Mouschovias, T. Ch., & Ciolek, G. E. 1999, in The Origin of Stars and Planetary Systems, ed. C. J. Lada & N. D. Kylafis (Dordrecht: Kluwer), 305
Nakano, T. 1984, Fundam. Cosmic Phys., 9, 139
Scalo, J. M. 1985, in Protostars and Planets II, ed. D. C. Black & M. S. Matthews (Tucson: Univ. Arizona Press), 201
Shu, F. H. 1983, ApJ, 273, 202
Shu, F. H., Adams, F. C., & Lizano, S. 1987, ARA&A, 25, 23
Skrutskie, M. F., et al. 1997, in The Impact of Large Scale Near-IR Sky Surveys, ed. F. Garzon, N. Epchtein, A. Omont, W. B. Burton, & P. Persi (Dordrecht: Kluwer), 25
Tachihara, K., Mizuno, A., & Fukui, Y. 2000, ApJ, 528, 817
Williams, J. P., de Geus, E. J., & Blitz, L. 1994, ApJ, 428, 693
Zweibel, E. G. 2002, ApJ, 567, 962